Acta Crystallographica Section D
Biological Crystallography
ISSN 0907-4449

The structure of the hexagonal crystal form of hen egg-white lysozyme

C. Brinkmann,[a]* M. S. Weiss[b] and E. Weckert[a]

[a]HASYLAB at DESY, Notkestrasse 85, 22607 Hamburg, Germany, and [b]EMBL, Notkestrasse 85, 22607 Hamburg, Germany

Correspondence e-mail: christian.brinkmann@desy.de

Received 18 October 2005
Accepted 6 January 2006

PDB Reference: hexagonal hen egg-white lysozyme, 2fbb, r2fbbsf.

The three-dimensional structure of hen egg-white lysozyme (HEWL) in a hexagonal crystal form has been determined and refined to 1.46 Å resolution. This hexagonal crystal form crystallizes from a saturated sodium nitrate solution at pH 8.4. The crystals belong to space group $P6_122$, with unit-cell parameters $a = b = 85.64$, $c = 67.93$ Å. A total of 165 water molecules, 16 nitrate ions and five sodium ions were located in the electron-density map. The hexagonal crystal form exhibits a higher solvent content and a higher degree of disorder than other crystal forms of lysozyme. The flexibility of the protein depends on the crystal packing, although some residue ranges are flexible in all native HEWL crystal forms.

1. Introduction

Hen egg-white lysozyme (HEWL) is the most studied protein in biological crystallography (see Vaney *et al.*, 1996, and references therein) because of its stability, solubility and ease of crystallization under different conditions and in different crystal forms (Steinrauf, 1959). The first crystal structure of HEWL was solved by Blake *et al.* (1965) based on crystals belonging to the tetragonal space group $P4_32_12$. Subsequently, the crystal structure of HEWL was also solved in triclinic (Steinrauf, 1959; Ramanadham *et al.*, 1990; Hodsdon *et al.*, 1990; Vaney *et al.*, 1996; Walsh *et al.*, 1998), monoclinic (Alderton & Fevold, 1946; Crick, 1953; Steinrauf, 1959; Rao *et al.*, 1983; Harata, 1994; Vaney *et al.*, 1996, 2001) and orthorhombic (Alderton & Fevold, 1946; Haas, 1967; Berthou *et al.*, 1983; Vaney *et al.*, 1996) forms. Surprisingly, the structure of the hexagonal HEWL crystal form has not been described to date, despite the fact that crystallization conditions for this crystal form were reported almost 40 years ago (Haas, 1967).

The related enzymes turkey egg-white lysozyme (TEWL) and guinea fowl egg-white lysozyme (GEWL) have also both been crystallized in a hexagonal crystal form (Parsons, 1988; PDB code 2lz2, M. R. Parsons & S. E. V. Phillips, unpublished work, PDB code 3lz2, Howell *et al.*, 1992; PDB code 1tew, Howell, 1995; PDB code 1hhl, Lescar *et al.*, 1994). Whilst both crystallize in space group $P6_122$, only the unit-cell parameters of GEWL are similar to those of hexagonal HEWL.

Here, we report the crystal structure of hexagonal HEWL at 10 K and present some typical features of the hexagonal form compared with the triclinic, monoclinic, orthorhombic and tetragonal crystal forms (Brinkmann *et al.*, 2006). In order to elucidate the role of the different amino-acid sequences in crystal packing and flexibility, the hexagonal crystal form of HEWL (this study) was also compared with the hexagonal crystal forms of TEWL (Howell *et al.*, 1992; Howell, 1995) and GEWL (Lescar *et al.*, 1994).

Table 1
Data-collection and refinement statistics.

Values in parentheses are for the highest resolution shell.

Data collection	
No. of crystals	1
Wavelength (Å)	0.8043
Total rotation range (°)	180 + 180
Unit-cell parameters	
a (Å)	85.64
c (Å)	67.93
Resolution limits (Å)	70–1.46 (1.47–1.46)
Total no. of reflections	601049
Total no. of unique reflections	26081
Redundancy	23.0
Completeness (%)	100 (100)
$I/\sigma(I)$	77.6 (3.5)
$R_{\rm merge}$† (%)	3.8 (88.4)
$R_{\rm r.i.m.}$‡ (%)	3.9 (93.6)
$R_{\rm p.i.m.}$§ (%)	0.7 (25.5)
Overall *B* factor from Wilson plot (Å^2)	22.0
Refinement	
Resolution limits (Å)	51–1.46
Data cutoff [$F/\sigma(F)$]	0.0
Total no. of reflections¶	25544
No. of reflections in working set	25016
No. of reflections in test set	528
R†† (%)	18.3
$R_{\rm free}$ (%)	19.8 (26.0)
No. of amino-acid residues	129
No. of protein atoms	1010
No. of sodium ions	5
No. of nitrate ions	16
No. of water molecules	165
Ramachandran plot, core (%)	87.6
Ramachandran plot, allowed (%)	12.4
Ratio of observations + restraints to parameters	6.6
Average *B* factor of all atoms‡‡ (Å^2)	30.3
Average *B* factor of protein atoms (Å^2)	28.2
Average *B* factor of solvent atoms (Å^2)	39.0
R.m.s.d. bonds (Å)	0.021
R.m.s.d. angles (°)	2.0

† $R_{\rm merge} = \sum_{hkl}\sum_i |I_i(hkl) - \overline{I(hkl)}|/\sum_{hkl}\sum_i I_i(hkl)$, where $\sum_{hkl}$ denotes the sum over all independent reflections and $\sum_i$ the sum over all equivalent and symmetry-related reflections (Stout & Jensen, 1968). ‡ $R_{\rm r.i.m.} = \sum_{hkl}[N/(N-1)]^{1/2}\sum_{hkl}\sum|I_i(hkl) - \overline{I(hkl)}|/\sum_{hkl}\sum_i I_i(hkl)$ (Weiss & Hilgenfeld, 1997; Diederichs & Karplus, 1997; Weiss, 2001), where N enumerates the number of times a given reflection has been observed. § $R_{\rm p.i.m.} = \sum_{hkl}[1/(N-1)]^{1/2}\sum_{hkl}\sum|I_i(hkl) - \overline{I(hkl)}|/\sum_{hkl}\sum_i I_i(hkl)$ (Weiss & Hilgenfeld, 1997; Weiss, 2001). ¶ *TRUNCATE* uses the following criteria for rejecting reflections: $I_{\rm obs} < -3.7\ {\rm SD}_{\rm obs}$ or $I_{\rm obs} < ({\rm SD}_{\rm obs})^2/\langle I\rangle - 4\ {\rm SD}_{\rm obs}$. For the discussed hexagonal HEWL structure, about 500 reflections were rejected by *TRUNCATE*. †† $R = \sum_{hkl}|F_{\rm obs} - kF_{\rm calc}|/\sum_{hkl}F_{\rm obs}$. ‡‡ TLS parameters: *T*, −0.213, −0.062, −0.119, −0.005, 0.049, −0.090; *L*, 4.06, 1.11, 2.46, 0.52, 1.07, 0.33; *S*, −0.107, 0.176, 0.020, 0.140, −0.093, −0.124, −0.054, 0.406.

2. Materials and methods

HEWL was crystallized in its hexagonal crystal form following the protocol described in detail in Haas (1967). Briefly, commercially available hen egg-white lysozyme (Merck; EC 3.2.1.17; K29564981) was purified using gel-filtration chromatography. For this purpose, a 10%(*v*/*v*) acetonic lysozyme solution was loaded onto a HiLoad 16/60 Superdex 75pg column (Amersham Biosciences; flow rate 1.5 ml min^{-1}; temperature 293 K). The protein was eluted in 1 ml fractions. For each fraction, the UV absorption (280 nm) was measured using an ÄKTA prime device (Amersham Biosciences). The ten fractions with the highest protein content were analyzed by SDS–PAGE (EPS 301 and Hoefer SE 245, Amersham Biosciences). The five fractions containing the purest protein material were pooled, filtrated and concentrated to a final concentration of 183 mg ml^{-1}. The concentration of the purified lysozyme solution was measured by UV absorption. For crystallization, solid sodium bicarbonate was added to a 10%(*v*/*v*) aqueous acetone solution until the pH value reached 8.4. The solution was then saturated with sodium nitrate. Concentrated lysozyme solution was then added to this solution to a final concentration of 25 mg ml^{-1}. The crystallization temperature was 293 K.

Diffraction data collection was carried out at synchrotron beamline X13 at EMBL Hamburg, Germany. The cryoprotected (Paratone-N; HR2-643, Hampton Research) crystal was flash-cooled in a helium stream to a temperature of 10 K using an Oxford Diffraction Helijet. Intensity data were collected using a MAR CCD detector (165 mm). Two sets of data each consisting of 180° of rotation were collected at resolution cutoffs of 2.15 and 1.46 Å using different exposure times to cope with saturated detector pixels. The data were integrated, scaled and merged using the programs *DENZO* and *SCALEPACK* (Otwinowski, 1993; Otwinowski & Minor, 1997). The redundancy-independent merging *R* factor $R_{\rm r.i.m.}$ and the precision-indicating merging *R* factor $R_{\rm p.i.m.}$ were calculated using the program *RMERGE* (available from www.embl-hamburg.de/~msweiss/project/msw_qual.html or from MSW upon request). Structure-factor amplitudes were obtained applying the method of French and Wilson as implemented in the program *TRUNCATE* (Collaborative Computational Project, Number 4, 1994). Similar experiments were performed on crystals of HEWL in its triclinic, monoclinic, orthorhombic and tetragonal crystal form (Brinkmann *et al.*, 2006).

The PDB entry 1dpw (resolution 1.64 Å, $R = 17.83\%$; Weiss *et al.*, 2000) was used as a starting model for molecular replacement. After successfully rotating and translating the model using the program *MOLREP* (Collaborative Computational Project, Number 4, 1994), a rigid-body refinement was carried out with the program *REFMAC*5 (Collaborative Computational Project, Number 4, 1994). The structure was then refined to a resolution of 1.46 Å using the maximum-

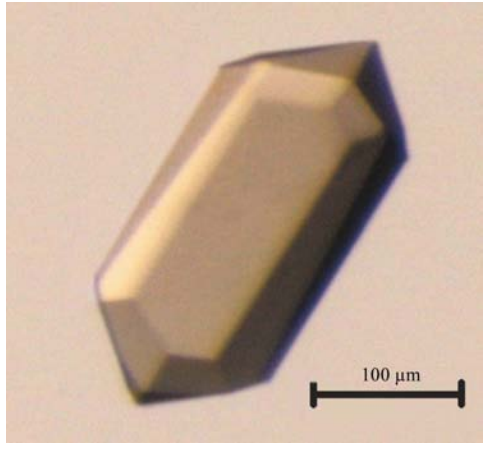

Figure 1
Single crystal of hexagonal hen egg-white lysozyme.

likelihood target function. The structure was verified using the program *XtalView* (McRee, 1999). Additional water molecules, nitrate and sodium ions were added, side chains were rebuilt in some places and further refinement cycles were performed until refinement converged. The refinement was then concluded with six TLS refinement cycles using the whole molecule as a rigid body followed by an additional 80 cycles, including isotropic temperature-factor refinement considering the obtained TLS parameters. Structure comparisons were carried out using the vector-superposition algorithm of Kabsch (1978) as implemented in the program *LSQKAB* (Collaborative Computational Project, Number 4, 1994). Crystal contacts were calculated with the program *CONTACT* (Collaborative Computational Project, Number 4, 1994). The distance criterion for a contact was defined to be less than 3.6 Å. For water-mediated contacts a *B*-factor cutoff of 30 Å^2 was applied to the water molecules. The program *ANISOANL* (Collaborative Computational Project, Number 4, 1994) was used to analyze the *B* values of the structure.

3. Results and discussion

3.1. Crystallization, diffraction data collection and refinement

As described in Haas (1967), hen egg-white lysozyme obtained at pH 8.4 in the presence of sodium nitrate crystallizes in hexagonal idiomorphic dipyramidial prisms of maximum dimensions of up to 1.0 × 0.5 × 0.5 mm within a few days. The typical crystal shape of the hexagonal crystal form is presented in Fig. 1. Relevant details of data collection and processing are given in Table 1. The hexagonal crystal form diffracts less well than other HEWL crystal forms at the same temperature, comparable crystal size, exposure time and experimental efforts. Nevertheless, the high quality of the data set is evident from the values presented. In spite of the choice of resolution cutoff [$I/\sigma(I) \geq 3.5$], the $R_{\rm merge}$ parameter of the outer shell is quite high (∼88%). This may in part be explained by the high redundancy of the data of about 23. However, the high redundancy also leads to a value for $R_{\rm p.i.m.}$ of 26% in the outer resolution shell. Since $R_{\rm p.i.m.}$ describes the precision of the averaged intensities (see Weiss, 2001), it is clear that significant information is still present at the high-resolution limit. This notion is corroborated by the low free-*R* factor of 26% in the outer resolution bin.

The refinement statistics are also given in Table 1. The *R* value drops from 22.4 to 18.3% and the $R_{\rm free}$ value drops from 25.4 to 19.8%, respectively, when a TLS refinement is performed. This observation hints at a comparatively high degree of static disorder in the hexagonal crystal form.

3.2. Quality of the protein structure

All 129 amino acids can be fitted to the electron-density map. However, smeared electron density hampers distinct assignment of the course of the main chain in the chain segments Pro70–Gly71 and Asp101, indicating the possibility of multiple main-chain conformations. The electron density of the side chains Arg21, Arg45, Arg61, Lys97, Asn103 and Arg128 was found to be truncated. As described in the literature for other HEWL crystal forms (Howell, 1995; Walsh *et al.*, 1998) the electron densities of several arginine residues are truncated if they are not involved in a crystal contact, which can be regarded as a high degree of mobility of the side chain. Two alternative conformations can be modelled for the side chains of Asn19 and Asp119.

As listed in Table 1, the r.m.s. deviations of the ideal bond lengths and ideal bond angles are comparable to those of other HEWL crystal forms (Vaney *et al.*, 1996, 2001; Walsh *et al.*, 1998; Weiss *et al.*, 2000) and to hexagonal TEWL (Parsons, 1988; PDB code 2lz2, M. R. Parsons & S. E. V. Phillips, unpublished; Howell *et al.*, 1992; Howell, 1995) and GEWL (Lescar *et al.*, 1994).

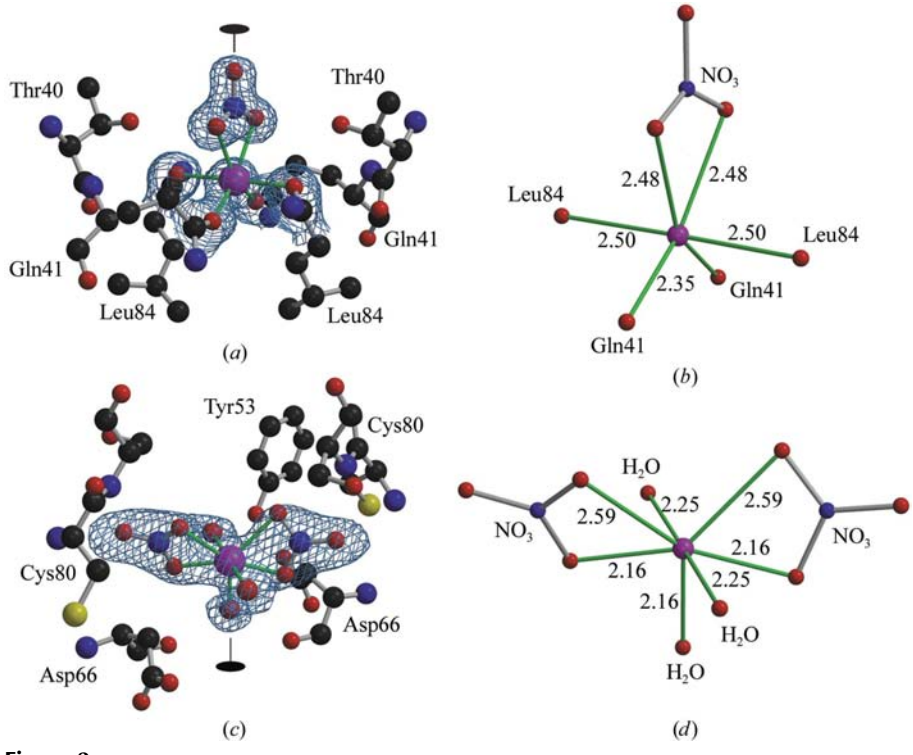

Figure 2
(*a*) and (*b*) Na132 and (*c*) and (*d*) Na133 in the hexagonal HEWL crystal form. The twofold symmetry axes are indicated. The distances between sodium and connected O atoms are shown in (*b*) and (*d*), respectively. ($2F_{\rm o} - F_{\rm c}$) maps contoured at 1.0σ. Distances are given in Å. Figures were generated using *MOLSCRIPT* v2.1.2 (Kraulis, 1991), *BOBSCRIPT* (Esnouf, 1997) and *RASTER3D* v2.7b (Merritt & Bacon, 1997).

Table 2
Structural superpositions of HEWL.

(*a*) Structural superposition of HEWL in different crystal forms (triclinic, monoclinic, orthorhombic and tetragonal structures; Brinkmann *et al.*, 2006). Tcl, triclinic ($P1$); mcl-A/B, monoclinic, molecule *A*/*B* ($P2_1$); ortho, orthorhombic ($P2_12_12_1$); tetr, tetragonal ($P4_32_12$); hexa, hexagonal ($P6_122$). In the upper triangle the r.m.s. deviations are given based on all 129 superimposed C^{α} pairs, whereas in the lower triangle the chain segments 45–50, 68–73 and 97–104 were excluded.

	tcl	mcl-A	mcl-B	ortho	tetr	hexa
tcl	—	0.75	0.75	0.66	0.69	1.27
mcl-A	0.46	—	0.68	0.63	0.38	1.10
mcl-B	0.52	0.53	—	0.83	0.71	1.21
ortho	0.41	0.49	0.59	—	0.58	1.14
tetr	0.35	0.36	0.50	0.44	—	1.07
hexa	0.62	0.52	0.55	0.61	0.53	—

(*b*) Structural superposition of hexagonal HEWL, GEWL (Lescar *et al.*, 1994) and TEWL (PDB code 3lz2, Howell *et al.*, 1992; PDB code 1tew, Howell, 1995). In the upper triangles all C^{α} pairs are involved in the calculations, whereas in the lower triangle residues 70–71 and 101–102 were excluded. Calculations were performed using the program *LSQKAB* (Collaborative Computional Project, Number 4, 1994).

	HEWL	GEWL	1tew	3lz2
HEWL	—	1.16	0.95	1.05
GEWL	0.79	—	0.93	0.87
1tew	0.64	0.86	—	0.56
3lz2	0.71	0.80	0.52	—

3.3. Sodium and nitrate ions

Each of the five localized sodium ions is connected to at least one nitrate ion. Sodium ion Na131 bonds to Ser60 O, Cys64 O, Ser72 OG, Arg73 O, one water molecule and one nitrate ion. An identical sodium-ion position within the loop of residues 60–74 has previously been described for the monoclinic, orthorhombic and tetragonal crystal forms of HEWL, but no such position was found in the triclinic form (*e.g.* Walsh *et al.*, 1998; Harata & Akiba, 2004; Vaney *et al.*, 1996, 2001; Brinkmann *et al.*, 2006). Sodium ion Na132 is located on a twofold axis and is connected to two O atoms of a nitrate ion located on the same twofold axis, Gln41 OE1, Leu84 O and symmetry-equivalent atoms (see Fig. 2). Na133 is also located on a twofold axis and is sevenfold coordinated by two nitrate ions and three water molecules (see Fig. 2). Na134 binds to Arg114 O, Arg14 O, one nitrate ion and two water molecules. Na135 bonds to two nitrate ions. Two sodium ions, Na132 and Na134, form crystal contacts *via* bridging sodium ions (Gln41–Na132–Gln41 and Leu84–Na132–Leu84, Arg114–Na134–Arg14) and Na133 generates a nitrate–water complex which also acts as a bridge between two symmetry-related lysozyme molecules (see Fig. 2). In the hexagonal HEWL structure, a total of 16 nitrate ions could be observed. They are located at sodium ions with a minimum distance of 2.2 Å and at peptide N atoms as well as at the Arg NH1,2, Arg NE, Lys NZ, Asn ND2, His ND1, Asp OD1,2, Ser OG and Thr OG1 atoms with a minimum distance of 2.7 Å. Additionally, ten nitrate ions are bound at a crystal contact between two lysozyme molecules and all nitrate ions are coordinated by water molecules. In comparison to the hexagonal structure, the lysozyme molecule in the triclinic packing exhibits three identical nitrate positions, namely NO3 154, NO3 155 and NO3 163 (NO3 notation refers to PDB code 2fbb), and in the monoclinic packing five nitrate positions (NO3 153, NO3 154, NO3 156, NO3 161, NO3 163; NO3 notation refers to PDB code 2fbb) are indentical (Brinkmann *et al.*, 2006).

3.4. Comparison with other HEWL crystal forms and with TEWL and GEWL

Table 2(*a*) lists the r.m.s. coordinate displacement values for C^{α} atoms for the tetragonal, orthorhombic, monoclinic and triclinic structures (Brinkmann *et al.*, 2006, structures observed under the same conditions as for the hexagonal form) and the hexagonal crystal form (see also Fig. 3). Main deviations are determined by the differences of the three flexible loop regions defined by residues 45–50, 68–73 and 97–104. The region 97–104 in particular appears to be distinctly different in the hexagonal crystal form compared with all other crystal forms. Omitting these highly flexible regions from the comparison produces r.m.s. deviations which are very similar between the various HEWL crystal forms. It turns out that the

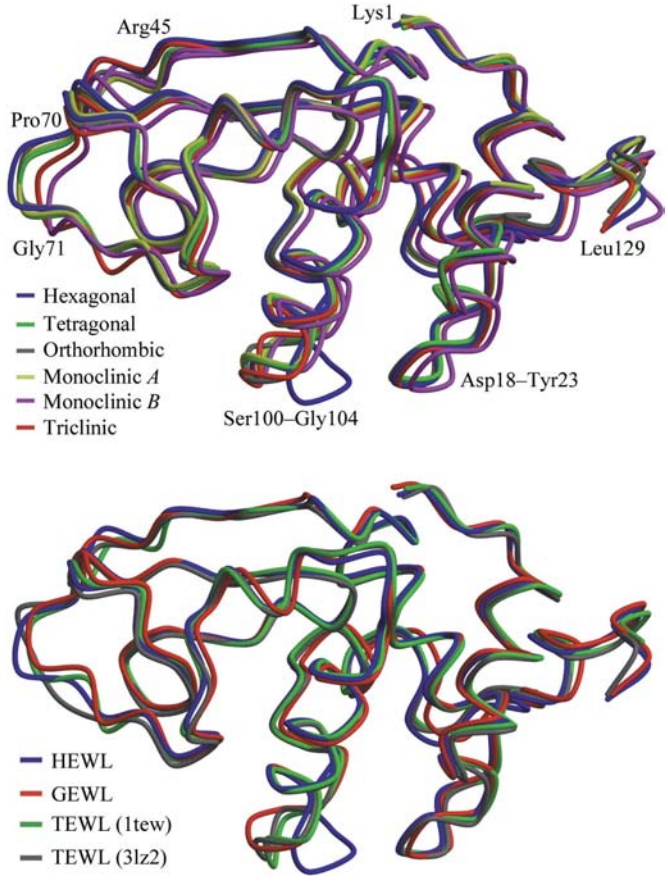

Figure 3
C^{α} superposition of HEWL crystal forms (triclinic, monoclinic, orthorhombic and tetragonal structures; Brinkmann *et al.*, 2006) and of HEWL, GEWL and TEWL. Calculations were performed using the program *LSQKAB* (Collaborative Computional Project, Number 4, 1994). Figures were generated using *MOLSCRIPT* v2.1.2 (Kraulis, 1991).

Table 3
Intermolecular distances less than 3.6 Å in the hexagonal HEWL structure calculated with *CONTACT* (Collaborative Computional Project, Number 4, 1994).

Similar contacts, *i.e.* contacts between the same amino-acid numbers in hexagonal GEWL (Howell, 1995) and TEWL (Lescar *et al.*, 1994) are also shown. Water contacts are ignored to keep the list manageable.

Atom–atom contact	HEWL	GEWL	TEWL
Lys1 N—Ser86 OG^{i}	2.99	—	—
Gln41 NE2—Ser81 O^{i}	2.90	—	—
Gln41 OE1—Leu84 O^{i}	3.26	—	—
Gln41 OE1—Ser85 N^{i}	3.34†	—	—
Asp66 O—Arg68 NH1^{i}	3.19	—	—
Lys13 NZ—Asp119 OD1^{ii}	3.17	—	—
Lys13 NZ—Asp119 OD2^{ii}	2.80	—	—
Arg14 NH2—Ala/Val122 O^{ii}	2.97	2.93	—
His15 O—Arg114 NH1^{ii}	3.06	—	—
Leu15 O—Arg114 NH2^{ii}	—	—	3.27
Lys96 NZ—Arg114 NH1^{ii}	3.42†	—	—
Lys96 NZ—Arg114 NH2^{ii}	—	—	3.26
Asn19 ND2—Gly22 O^{iii}	2.87	—	—
Asn19 OD1—Asn19 OD1^{iii}	3.32†	—	—
Asp48 O—Arg112 NH2^{iv}	3.02	—	—
Arg61 NH1—Ala107 O^{iv}	3.47†	—	—
Trp62—Trp62^{iv}‡	∼3.3	∼3.6	—
Pro70 O—Asn106 O^{iv}	3.50†	—	—
Arg73 NH1—Ile98 O^{iv}	—	2.85	—
Arg73 NH2—Ile98 O^{iv}	2.90	3.03	—
Arg125 NE—Cys127 O^{v}	3.16	—	—
Arg125 NH2—Cys127 O^{v}	2.96	—	—
Lys125 NZ—Cys127 O^{v}	—	2.81	—
Arg125 NH2—Arg128 NH1^{v}	3.43†	—	—
Lys125 NZ—Arg128 O^{v}	—	2.76	—

Symmetry codes: (i) $x-y,-y,-z$, (ii) $x-y,x,z+1/6$, (iii) $x,x-y,-z+1/6$, (iv) $-x+y,y,-z+1/2$, (v) $y,-x+y,z+5/6$. † Weak contact. ‡ Stacking contact of Trp.

conformation of the lysozyme molecule is similar in different packings, excluding highly flexible areas. In Table 2(*b*) the r.m.s. coordinate deviations in C^{α}-atom positions are shown for the hexagonal crystal forms of the whole molecule (upper triangle) and of the subset of atoms which are most clearly defined in the electron-density map (lower triangle). Again, the largest difference between the three structures is located in the loop 97–104. Fig. 3 depicts the superposition of C^{α} atoms of HEWL, GEWL and TEWL.

3.5. Comparison of the crystal packing of HEWL with TEWL and GEWL

The crystal packing of all hexagonal structures mentioned in this report can be described by space group $P6_122$. The unit-cell parameters are similar in HEWL (a = 85.6, c = 67.9 Å, resolution limit = 1.46 Å) and GEWL (a = 89.2, c = 61.7 Å, resolution limit = 1.90 Å; Lescar *et al.*, 1994), but differ in TEWL (PDB code 1tew: a = 71.0, c = 83.0 Å, resolution limit 1.65 Å, Howell, 1995; PDB code 3lz2: a = 70.9, c = 84.6 Å, resolution limit 2.50 Å, Howell *et al.*, 1992). In Table 3 all contacts between atoms of symmetry-related lysozyme molecules in hexagonal HEWL are listed. In addition, if the equivalent amino acids in GEWL and TEWL (PDB code 1tew) are involved in crystal contacts, these are also listed. As well as the unit-cell parameters, the crystal contacts in hexagonal HEWL and GEWL are also comparable (see Table 3) despite the 11 amino acids that differ between HEWL and GEWL (HEWL→GEWL: Thr40→Ser, Ile55→Val, Leu84→

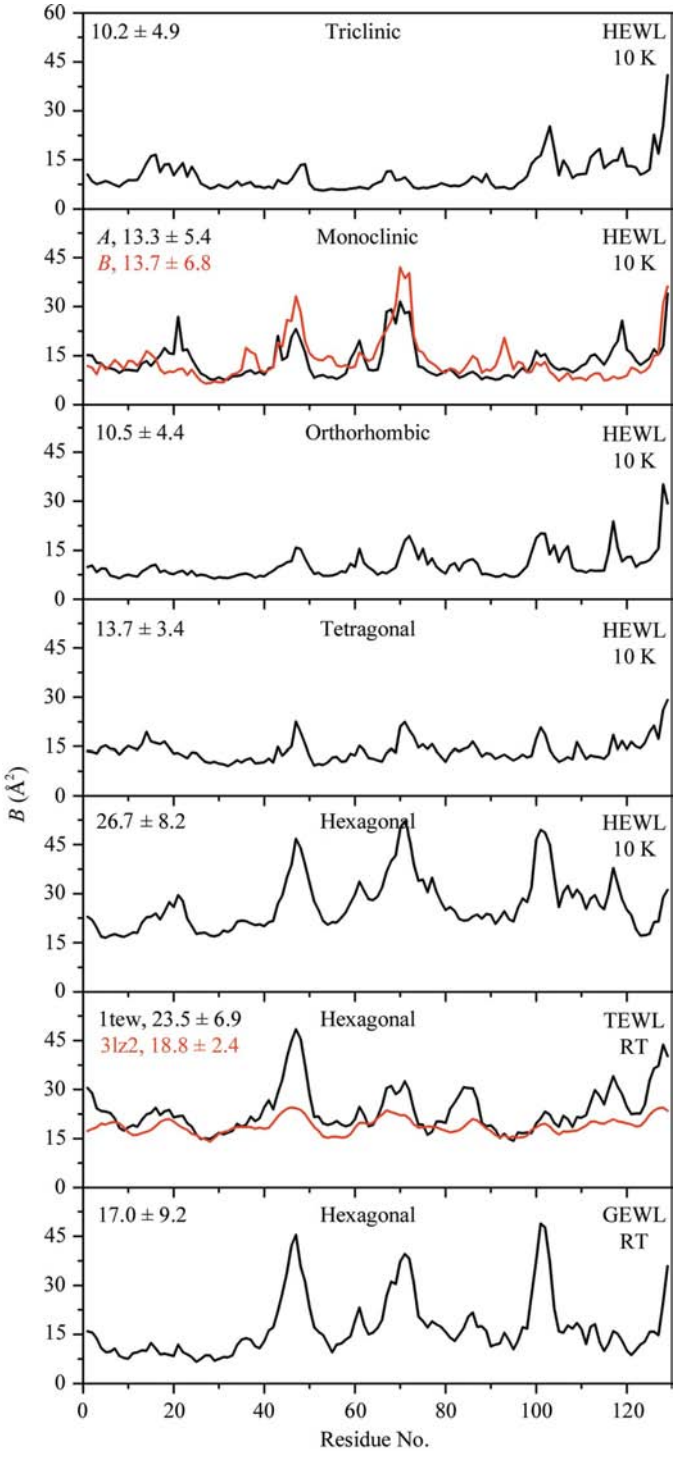

Figure 4
Plot of average main-chain B factors *versus* residue number for HEWL crystal forms (triclinic, monoclinic, orthorhombic and tetragonal structures; Brinkmann *et al.*, 2006) and of hexagonal GEWL and TEWL (for TEWL black = 1tew, red = 3lz2). The mean B value of each crystal form is given on the left ± standard deviation. The structure of GEWL was published by Lescar *et al.* (1994) (1hhl) and the TEWL structures by Howell *et al.* (1992) (3lz2) and Howell (1995) (1tew).

Gln, Ser91→Thr, Val92→Ala, Asn103→Asp, Asn113→Lys, Arg114→His, Gln121→Arg, Ala122→Val, Arg125→Lys). Each molecule in the crystal lattice has five other molecules in its immediate vicinity. Whereas in HEWL 29 amino acids are found to be involved in 19 hydrogen bonds and one aromatic stacking interaction, only 13 amino acids form ten crystal contacts in GEWL, indicating a much looser packing. In addition, 13 solvent-ion and six water-mediated contacts were observed in the hexagonal form of HEWL, but only ten water-mediated contacts were found in GEWL. Of the 11 amino acids that differ between HEWL and GEWL, four are involved in crystal contacts in HEWL and two in GEWL. Five contacts are similar in HEWL and GEWL (Table 3). Although HEWL and TEWL are closer in amino-acid sequence than HEWL and GEWL (only seven amino acids differ between HEWL and TEWL: Phe3→Tyr, His15→Leu, Gln41→His, Arg73→Lys, Val99→Ala, Asp101→Gly, Gln121→His), the overall arrangement of HEWL in the hexagonal packing is quite different from the hexagonal crystal form of TEWL. Of the amino acids which differ between HEWL and TEWL, three are involved in HEWL crystal contacts and two in TEWL crystal contacts. Moreover, two contacts in TEWL involving the guanidinium group of Arg114 are similar to those in HEWL. In spite of different crystallization conditions (PDB code 3lz2: ammonium acetate buffer pH 8 and NaCl; 1tew: sodium acetate buffer pH 4.5 and KSCN; Howell *et al.*, 1992; Howell, 1995), the packings of the two TEWL forms are practically identical. Similar behaviour has also been observed for tetragonal HEWL crystallized at pH 4.5 and pH 8.0 (Weiss *et al.*, 2000).

In summary, HEWL and GEWL crystallize in practically identical molecular packings despite the fact that 11 amino acids are different. In contrast, the packings of HEWL and TEWL are different although only seven amino acids differ between the molecules.

3.6. Solvent content and disorder

Compared with all other crystal forms, the hexagonal form of HEWL exhibits a higher water content (triclinic, 28%; monoclinic, 30%; orthorhombic, 40%; tetragonal, 37%; hexagonal, 51%) and in addition fewer crystal contacts per molecule (triclinic, ∼100; monoclinic, ∼80; orthorhombic, ∼80; tetragonal, ∼70; hexagonal, ∼40). Along with the higher water content and fewer crystal contacts, increased static disorder can be observed, which can be interpretated as a higher flexibility of lysozyme in the hexagonal packing. In Fig. 4, the average main-chain B values are plotted for all native HEWL crystal forms and for the hexagonal GEWL and TEWL forms. Compared with other crystal forms, the hexagonal crystal forms reveal a higher mean B value, *i.e.* a higher degree of static disorder. The highest B values within the hexagonal HEWL structure are at residues 45–50, which are in between two β-strands, residues 68–73, which are involved in a loop between an α-helix and a β-strand, and residues 16–25, 97–104 and 118–120, which are loops connecting two α-helices. The correlation coefficient between the averaged main-chain B factors between hexagonal HEWL and all other HEWL crystal forms and TEWL and GEWL are listed in Table 4. Except for the triclinic crystal form, the correlation coefficients calculated with residue ranges 45–50, 68–73 and 97–104 excluded are in general lower than the correlation factor including all residues. These flexible regions can be observed to a greater or lesser extent in all other native crystal forms but in different packings, *i.e.* the crystal contacts clearly determine the extent of flexibility (see Fig. 4), especially for the triclinic packing. It turns out that the correlation of the averaged B values including all residues is low between the structure with the highest symmetry and the highest solvent content (hexagonal HEWL) and the structure with the lowest symmetry and the lowest solvent content (triclinic HEWL). The similar packing of HEWL and GEWL tends to a similar distribution of the B parameters, as described by the correlation parameter of 0.88.

Table 4
Correlation parameters.

Correlation parameter = $[\sum_i (x1_i - \langle x1\rangle)(x2_i - \langle x2\rangle)]/[\sum_i (x1_i - \langle x1\rangle)^2 \times \sum_i (x2_i - \langle x2\rangle)^2]^{1/2}$, where $\langle x1, 2\rangle = (\sum_i x1, 2)/i$.

(*a*) Correlation parameter of the averaged B values of HEWL in different crystal forms (triclinic, monoclinic, orthorhombic and tetragonal structures; Brinkmann *et al.*, 2006). Tcl, triclinic ($P1$); mcl-A/B, monoclinic, molecule A/B ($P2_1$); ortho, orthorhombic ($P2_12_12_1$); tetr, tetragonal ($P4_32_12$); hexa, hexagonal ($P6_122$). In the upper triangle the correlation parameter of the B values of all main-chain atoms are given, whereas in the lower triangle the B values of the main-chain atoms of the highly flexible residues 45–50, 68–73 and 97–104 were excluded.

	tcl	mcl-A	mcl-B	ortho	tetr	hexa
tcl	—	0.48	0.18	0.65	0.62	0.30
mcl-A	0.69	—	0.67	0.51	0.64	0.62
mcl-B	0.38	0.40	—	0.46	0.59	0.59
ortho	0.68	0.51	0.49	—	0.77	0.59
tetr	0.74	0.58	0.53	0.75	—	0.46
hexa	0.25	0.45	0.27	0.47	0.18	—

(*b*) Correlation parameter of the B values of hexagonal HEWL, GEWL (Lescar *et al.*, 1994) and TEWL (PDB code 3lz2, Howell *et al.*, 1992; PDB code 1tew, Howell, 1995). In the upper triangle the correlation parameter of the B values of the main-chain atoms are given, whereas in the lower triangle the B values of residues 70–71 and 101–102 have been excluded.

	HEWL	GEWL	1tew	3lz2
HEWL	—	0.88	0.43	0.48
GEWL	0.66	—	0.56	0.55
1tew	0.29	0.56	—	0.83
3lz2	0.36	0.52	0.78	—

4. Conclusions

The crystal structure of hexagonal HEWL has been determined and refined to high resolution and was compared with other native crystal forms as well as with hexagonal TEWL and GEWL. The main features of hexagonal HEWL are the clearly higher water content and disorder compared with all other native HEWL crystal forms, which indicate a higher flexibility of the lysozyme molecule in the hexagonal packing. In principle, the conformation of the protein in different packings is very similar and significant differences only arise in

highly flexible loop regions. Moreover, lysozyme in different packings exhibits explicit differences in flexibility. In addition, it turns out that a different amino-acid sequence influences the packing, but it appears that it depends on the particular nature of the exchanged amino acids.

We would like to thank the staff of the X-ray diffraction beamline X13 at EMBL (Hamburg, Germany) for support and beamtime. We would also like to acknowledge the help of Dr Garib Murshudov for his advice concerning TLS refinement in *REFMAC*. CB acknowledges support from the DESY Fellowship Program.

References

Alderton, G. & Fevold, H. L. (1946). *J. Biol. Chem.* **164**, 1–5.
Berthou, J., Lifchitz, A., Artymiuk, P. J. & Jollès, P. (1983). *Proc. R. Soc. London Ser. B*, **217**, 471–489.
Blake, C. C. F., Koenig, D. F., Mair, G. A., North, A. C. T., Phillips, D. C. & Sarma, V. R. (1965). *Nature (London)*, **206**, 757–761.
Brinkmann, C., Weiss, M. S. & Weckert, E. (2006). In preparation.
Collaborative Computational Project, Number 4 (1994). *Acta Cryst.* D**50**, 760–763.
Crick, F. H. C. (1953). *Acta Cryst.* **6**, 221–222.
Diederichs, K. & Karplus, P. A. (1997). *Nature Struct. Biol.* **4**, 269–275.
Esnouf, R. M. (1997). *J. Mol. Graph.* **15**, 132–134.
Haas, D. J. (1967). *Acta Cryst.* **23**, 666–667.
Harata, K. (1994). *Acta Cryst.* D**50**, 250–257.
Harata, K. & Akiba, T. (2004). *Acta Cryst.* D**60**, 630–637.
Hodsdon, J. M., Brown, G. M., Sieker, L. C. & Jensen, L. H. (1990). *Acta Cryst.* B**46**, 54–62.
Howell, P. L. (1995). *Acta Cryst.* D**51**, 654–662.
Howell, P. L., Almo, S. C., Parsons, M. R., Hadju, J. & Petsko, G. A. (1992). *Acta Cryst.* B**48**, 200–207.
Kabsch, W. (1978). *Acta Cryst.* A**34**, 827–828.
Kraulis, P. J. (1991). *J. Appl. Cryst.* **24**, 946–950.
Lescar, J., Souchon, H. & Alzari, P. M. (1994). *Protein Sci.* **3**, 788–798.
McRee, D. E. (1999). *J. Struct. Biol.* **125**, 156–165.
Merritt, E. A. & Bacon, D. J. (1997). *Methods Enzymol.* **277**, 505–524.
Otwinowski, Z. (1993). *Proceedings of the CCP4 Study Weekend. Data Collection and Processing*, edited by L. Sawyer, N. Isaacs & S. Bailey, pp. 56–62. Warrington: Daresbury Laboratory.
Otwinowski, Z. & Minor, W. (1997). *Methods Enzymol.* **276**, 307–326.
Parsons, M. R. (1988). PhD thesis. University of Leeds, England.
Ramanadham, M., Sieker, L. C. & Jensen, L. H. (1990). *Acta Cryst.* B**46**, 63–69.
Rao, S. T., Hoggle, J. & Sundaralingam, M. (1983). *Acta Cryst.* C**39**, 237–240.
Steinrauf, L. K. (1959). *Acta Cryst.* **12**, 77–79.
Stout, G. H. & Jensen, L. H. (1968). *X-ray Structure Determination. A Practical Guide*, p. 402. London: Macmillan.
Vaney, M. C., Broutin, I., Retailleau, P., Douangamath, A., Lafont, S., Hamiaux, C., Prangé, T., Ducruix, A. & Riès-Kautt, M. (2001). *Acta Cryst.* D**57**, 929–940.
Vaney, M. C., Maignan, S., Riès-Kautt, M. & Ducruix, A. (1996). *Acta Cryst.* D**52**, 505–517.
Walsh, M. A., Schneider, T. R., Sieker, L. C., Dauter, Z., Lamzin, V. S. & Wilson, K. S. (1998). *Acta Cryst.* D**54**, 522–546.
Weiss, M. S. (2001). *J. Appl. Cryst.* **34**, 130–135.
Weiss, M. S. & Hilgenfeld, R. (1997). *J. Appl. Cryst.* **30**, 203–205.
Weiss, M. S., Palm, G. J. & Hilgenfeld, R. (2000). *Acta Cryst.* D**56**, 952–958.